PREDICTING AND DETERMINING THE CONTACT PRESSURE DISTRIBUTION IN JOINTS FORMED BY V-BAND CLAMPS

M. Muller, S.M. Barrans
University of Huddersfield, Queensgate, Huddersfield HD1 3DH, UK

ABSTRACT

V-band clamps are utilised in a wide range of industries to connect together a pair of circular flanges, for ducts, pipes, turbocharger housings and even to form a joint between satellites and their delivery vehicle. In this paper, using a previously developed axisymmetric finite element model, the impact of contact pressure on the contact surface of the V-band clamp was studied and surface roughness measurements were used to investigate the distribution of contact pressure around the circumference of the V-band.

Keywords: V-band clamp, finite element model, surface roughness, contact analysis

1 INTRODUCTION

Focussing on elastic deformation during the assembling of V-band clamp joints, Shoghi et al. (2003) and Shoghi et al. (2004) generated finite element models and a classical analysis of the process. These were validated by the experimental tests of Shoghi et al. (2006). This work then led to recently published research by Barrans and Muller (2009) presenting an axisymmetric finite element model which analysed the failure mechanism of V-band joints, proving that the ultimate axial load capacity, was dependent on the clamp diameter. Based on their work, Muller and Barrans (2009) showed that during failure of a V-band joint for small clamp diameters the cross section deformed plastically into a non recovering state, whereas towards larger diameters a purely elastic deformation was observed. In a number of applications cracks have been observed propagating on the inner surface of the V-band close to the small internal radius generated during the roll forming process. In the same area the finite element model predicted a high concentration of plastic strain during failure of the V-band joint. With the same FE model the impact of flange geometry could be analysed and it was found by Muller and Barrans (2010) that the flange thickness in the contact area had the highest influence on the ultimate axial load capacity, drawing attention to the importance of considering manufacturing tolerances when designing such a joint. For all analytical or numerical models presented previously, the contact pressure between the flanges and the V-band clamp was assumed to be uniformly distributed. However, Shoghi (2003) showed that a non-uniform pressure distribution can be expected around the V-band. At that time it was not possible to measure the pressure distribution. This paper proposes to address this knowledge gap by using surface metrology to measure the permanent surface deformation generated by the contact pressure, and numerically investigate this by previously developed finite element models.

2 FINITE ELEMENT MODEL

Details about the set up of the finite element model can be taken from Muller and Barrans (2009), and are also shown in Figure 1. For the material, properties for AISI 304 stainless steel were taken from Shoghi et al. (2003), in which the Young's Modulus is 227GPa and the Poisson's Ratio is 0.29. The finite element package ABAQUS (v6.8) was employed to carry out the numerical analysis, which requires all stresses and strains to be given as true values. The yield stress σ_y was set to 648MPa and the true tensile strength σ_{tUTS} to 1182.7MPa. The finite element model presented here simulates a joint with a diameter of 235mm. The finite element model was set up to model the assembly and removal of the V-band clamp. The V-band is assembled by tightening the T-bolt nut with a certain Torque T_w, which generates a force F_β in the T-bolt and the radial direction of the V-band. Due to the wedging action of the V-section, this radial force generates the axial clamping load F_{ac}, pushing the flanges together. All of these three forces can be calculated using equations (1) to (3) taken from Shoghi (2003) and (4) taken from Shoghi et al. (2006), in which equation (4) is a modification of (3).

$$R_m = \left[\frac{d_1+d_2}{4}\right] \tag{1}$$

d_1 = inside diameter of the nut bearing surface
d_2 = outside diameter of the nut bearing surface
d_p = pitch diameter of the bolt
R_m = mean radius of the fastener under-head bearing surface

$$T_w = F_\beta \left[\frac{d_p}{2}\tan(\alpha_h + \lambda) + \mu_h R_m\right] \tag{2}$$

F_β = clamping load in the T-bolt
T_w = torque applied to the T-bolt
α_h = helix angle
μ_h = underhead coefficient of friction
λ = coefficient of friction of threads

$$F_\beta = \frac{F_{ac}\mu(\mu+tan\Phi)}{(1-\mu tan\Phi)(\mu cos\Phi+sin\Phi)}\left\{\frac{1}{1-e^{\frac{-\mu\beta}{\mu cos\Phi+sin\Phi}}}\right\} \tag{3}$$

$$F_{ac} = \frac{(1-\mu tan\Phi)F_\beta(\mu cos\Phi+sin\Phi)}{\mu(\mu+tan\Phi)}\left\{1-e^{\frac{-\mu\beta}{\mu cos\Phi+sin\Phi}}\right\} \tag{4}$$

F_{ac}= axial clamping force due to tightening of T-bolt nut
β= subtended angle of half the V-section
μ= coefficient of friction between the V-section band clamp and rigid flanges
Φ= angle of the V-section

Figures 2a and 2b show the simulated V-band contact zone after it has been taken off the flanges. In Figure 2a in which no friction has been assumed, almost no residual von-Mises stress can be seen at the surface. The peak stress lies under the surface. This phenomenon is due to the forces acting at the surface. Considering the von-Mises yield cylinder in three dimensional stress space, the two principal stresses acting in the plane of the surface will be compressive. The third principal stress is introduced by the contact force of the flange, acting directly normal to the surface and is again compressive. These three compressive stresses lead to a high hydrostatic stress and relatively small deviatoric stress, reducing the plastic strain and residual stress at the surface. This becomes clearer when taking into account friction as shown in Figure 2b (μ=0.2). Adding an extra shear stress at the surface, leads to larger residual stresses at the surface, and increases the peak stress by a ratio of about 3. This assumption is confirmed by Figures 3a and 3b, showing no plastic strain at the surface for the non friction case, and larger plastic strain at the surface for the case where friction has been included. A series of FE analyses undertaken for this paper have shown that with an axial clamping load, F_{ac}, below 30kN no plastic deformation in or close to the contact zone appears. With an axial clamping load of 30kN (23.6Nm) and depending on the coefficient of friction, plastic deformation would be present but would be hard to detect by surface roughness measurement. Even with an axial clamping load of 60kN (47.1Nm), the plastic deformation shown in Figures 4a and 4b is very small for both no friction and friction cases, and therefore hard to detect. However, the peak plastic strain has increased by approximately 2.5 when compared to 30kN. For the 60kN case, the influence of the hydrostatic stress and, for taking into account friction, the influence of shear stress on the plastic strain is similar to those of 30kN.

3 EXPERIMENTAL RESULTS

The surface roughness on the inside of the V-band was measured in ten zones, 5 equally distributed around each side of the V-section, in which the band is in contact with the flanges, to create a methodology which enables investigation of the contact pressure distribution around the inside of the V-band clamp. The purpose of this investigation is to show whether or not the contact pressure is distributed uniformly or non-uniformly around the circumference.

The set up of the V-band on the PGI stylus machine can be seen in Figure 5a, along with an example of the 25x25mm measured area shown in the red square in Figure 5b. Each band clamp was measured before and after assembly and the results for each area were compared to each other. Bands were assembled with torques T_w of 5, 10, 15 and 20Nm. It should be noted that the axial clamping loads of 30kN and 60 kN used in the FE simulation would have required T-bolt torques of 23.6 Nm and 47.1 Nm according to equations 1 to 4. These high torques are unrealistic and could not be applied to the sample bands.

An example measurement of one area close to the T-bolt can be seen in Figure 6a for the measured surface before assembling the band to the joint. The results shown in Figure 6b have been taken along the red line shown in Figure 6a. These figures were compared to Figures 6c and 6d after the assembly, and showed very little difference. Especially 6b and 6d seem to be slightly different but this is mainly due to the difficulty of always measuring the same line before and after assembly. Even small deviations in the measured position can give different results, and hence it is hard to directly compare the two diagrams. Comparing Figures 6a and 6b the roll forming process in which the band clamps are manufactured can clearly be identified, as the flat section (of the V-section) is clearly smother than the top part of the square, which represents the bent area and hence has a larger surface roughness. As no plastic deformation could be detected for the range of 5 to 20Nm, there seems to be only elastic deformation on the surface. This correlates very well with the findings of the finite element work in the previous section, in which plastic deformation could only be noticed from 30kN (23.6Nm), and even then the values were too small to be determinable. Another problem associated with this measurement type was marks and fringes appearing in the circumferential direction of the tested areas (Figures 7a and 7b). These were either due to table-noise and/or the preceding cold roll forming process used to manufacture these V-band clamps.

4 CONCLUSIONS

In this paper a previously developed axisymmetric finite element model for predicting the ultimate axial load capacity was utilised to numerically investigate the influence of contact pressure on the inner surface of a V-band clamp. The predictions showed very little plastic deformation in the contact area after the band clamp was assembled and then taken off again, even for torques that would never be reached in real applications.

The surface roughness measurements correlate well with the finite element analyses as it was not possible to pick up any plastic deformation of the inner contact surface. Moreover, table noise and the influences of the cold roll forming process highly affected the results and made it impossible to give reliable and accurate readings.

In the future finite element analysis of the cold roll forming process should be carried out to compare the residual plastic strains induced by manufacturing with the strains predicted in this paper, to see if either one of them is significantly smaller and, hence, can be neglected.

The measurement methodology should be improved to prevent table noise.

REFERENCES

Barrans, S.M., Muller, M., 2009. Finite element prediction of the ultimate axial load capacity of V-section band clamps. In: 7th International Conference on Modern Practice in Stress and Vibration Analysis, Cambridge, UK.

Muller, M., Barrans, S.M., 2009. Ultimate Axial Load Capacity of V-Band Clamp Joints. In: University of Huddersfield (Ed.), Proceedings of Computing and Engineering Annual Researchers' Conference, Huddersfield, UK, 14-18

Muller,M., Barrans,S.M., 2010. Impact of flange geometry on the ultimate axial load capacity of V-band clamps. In: 9th International Conference on Turbochargers and Turbocharging, London, UK.

Shoghi, K., 2003. Stress and strain analysis of flat and V-section band clamps. PhD thesis. University of Huddersfield.

Shoghi, K., Barrans, S.M., Rao, H.V., 2004. Stress in V-section band clamps. J. Mech. Eng. Sci. 218, part C, 251-261.

Shoghi, K., Barrans, S.M., Rao, H.V., 2003. Classical and finite element analysis of V-band retainers. In: NAFEMS World Congress, Orlando, Florida, USA.

Shoghi, K., Barrans, S.M., Ramasamy. P., 2006. Axial load capacity of V-section band clamp joints. In: 8th International Conference on Turbochargers and Turbocharging, London, UK, pp. 273-285

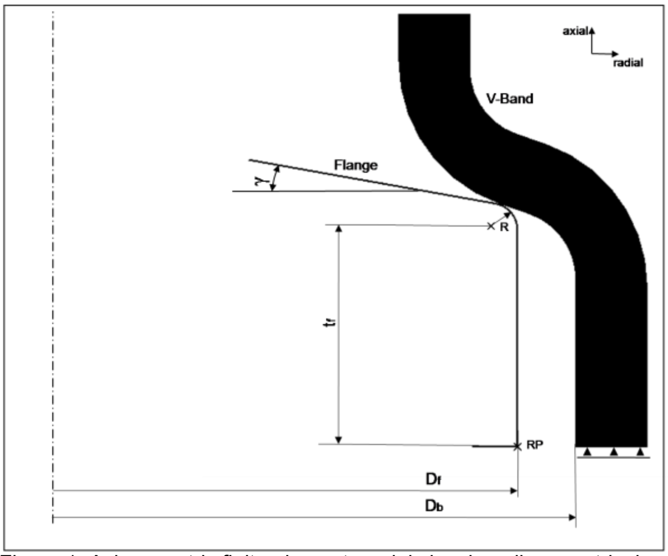

Figure 1: Axisymmetric finite element model showing all geometrical parameters, taken from Barrans and Muller (2009)

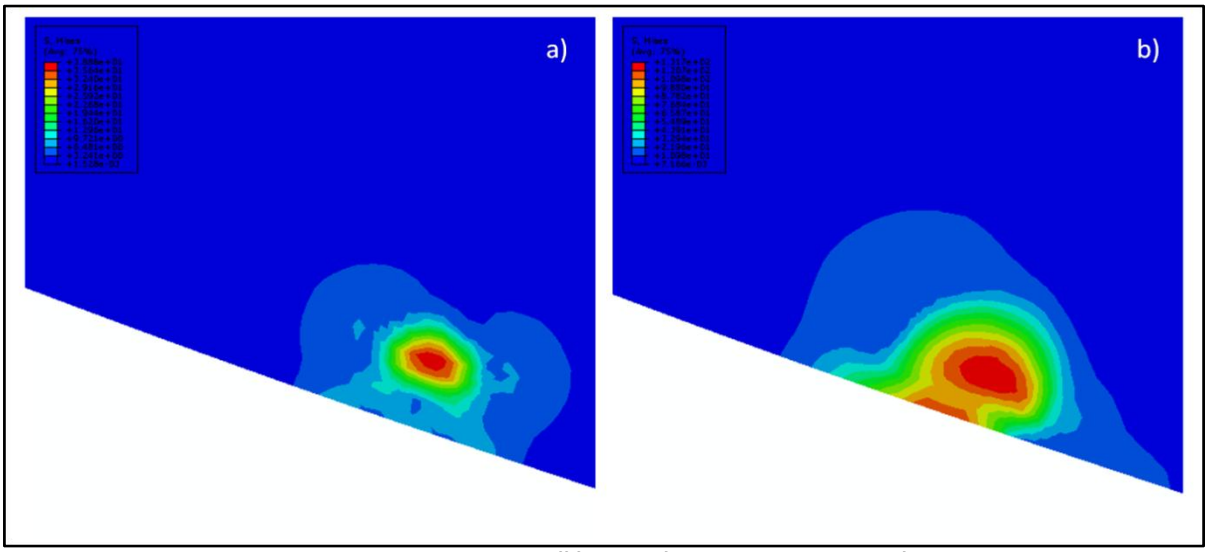

Figure 2: Residual stresses when V-band clamp is taken off flanges after axial clamping load of 60kN has been applied, a) μ=0, b) μ=0,2

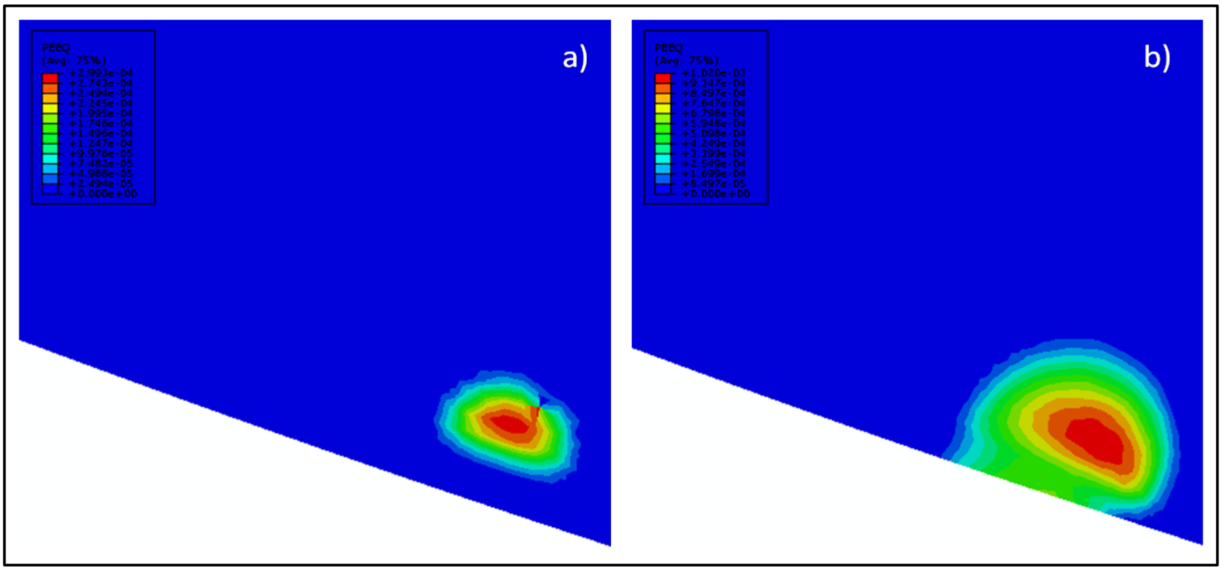

Figure 3: Plastic strains (PEEQ) when V-band clamp is taken off flanges after axial clamping load of 30kN has been applied, a) μ=0, b) μ=0,2

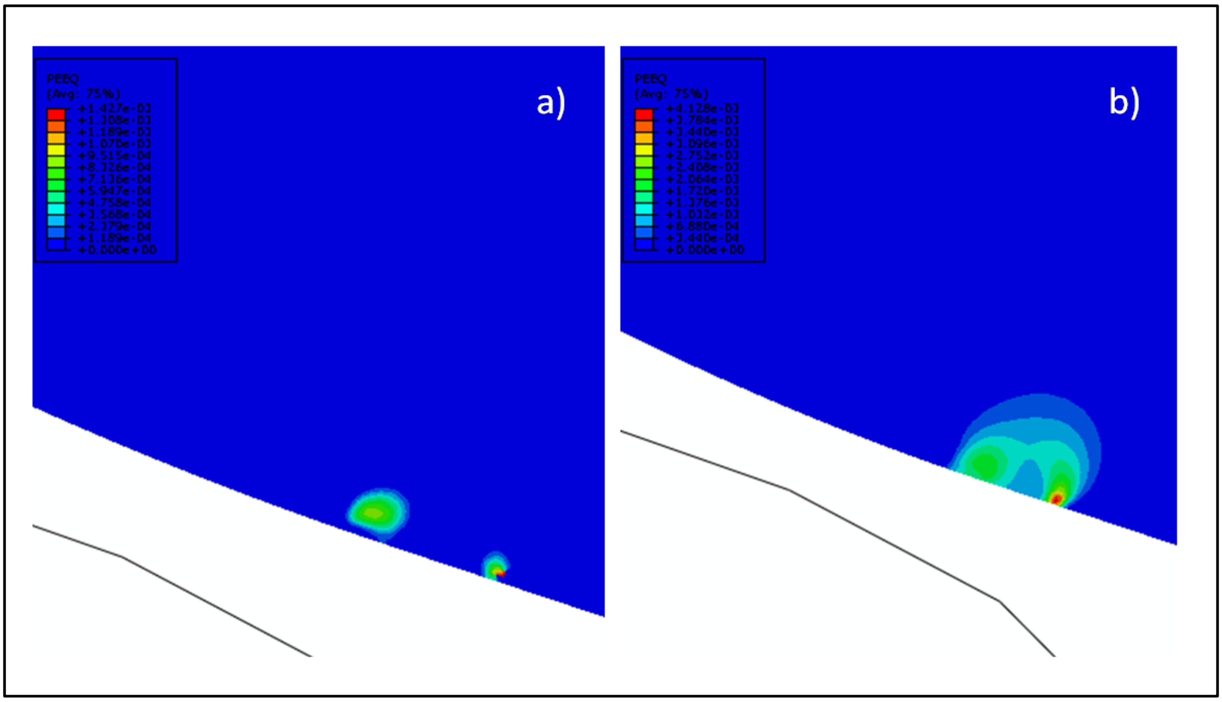

Figure 4: Plastic strains (PEEQ) when V-band clamp is taken off flanges after axial clamping load of 60kN has been applied, a) μ=0, b) μ=0,2

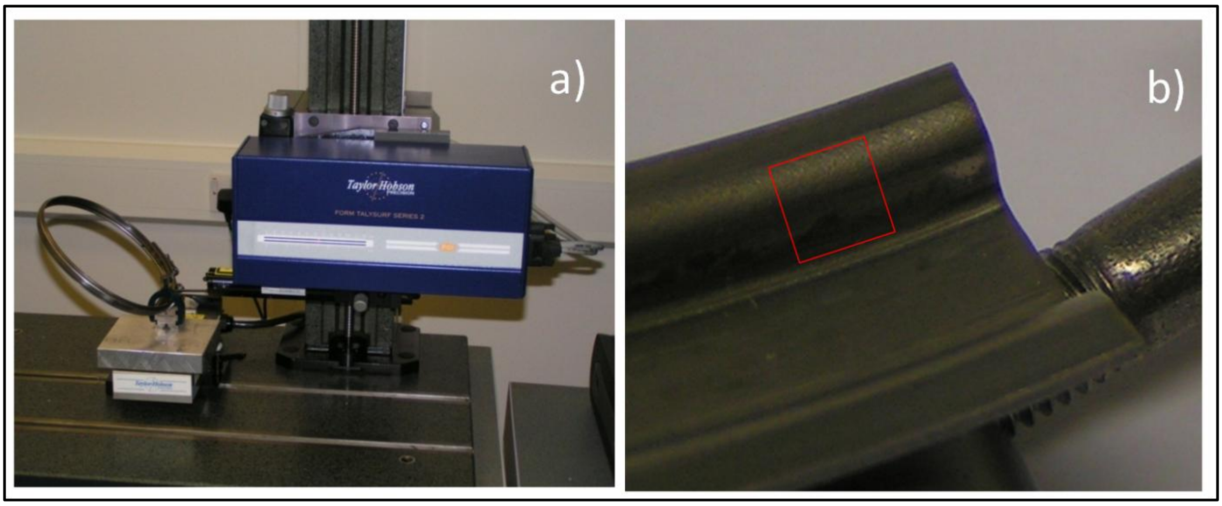

Figure 5: a) V-band measured on PGI stylus, b) Position of measured surface inside of V-band

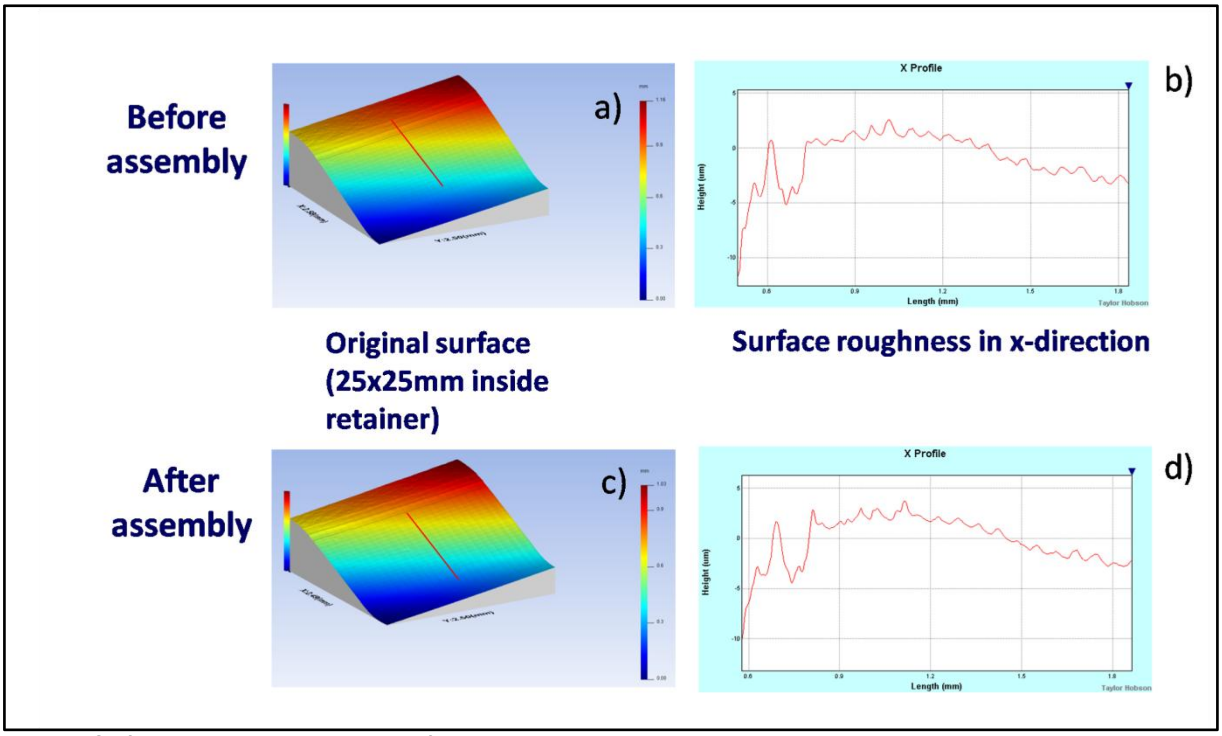

Figure 6: Surface roughness measurement of V-band

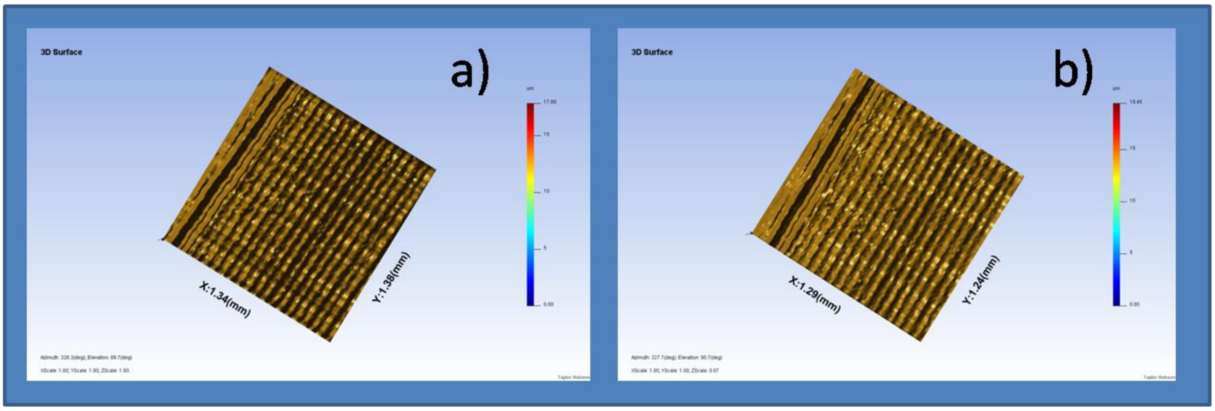

Figure 7: Surface measurements after levelling, a) before and b) after assembling